ACS Sustainable Chemistry & Engineering

Research Article

pubs.acs.org/journal/ascecg

s-Triazine Ring-Modified Waterborne Alkyd: Synthesis, Characterization, Antibacterial, and Electrochemical Corrosion Studies

Shabnam Pathan and Sharif Ahmad*

Materials Research Laboratory, Department of Chemistry, Jamia Millia Islamia,New Delhi-110025, India

Supporting Information

ABSTRACT: The surface coating industry is globally involved in developing useful, eco-friendly, and VOC (volatile organic compounds)-free coating systems, which exhibit promising physico-mechanical and corrosion protective performance. Herein, we report the synthesis of butylated melamine formaldehyde (BMF)-modified soy alkyd (SA-BMF). The structural elucidation and molecular weight of soy alkyd (SA) and SA-BMF resin was carried out by FT-IR, ^{1}H NMR, and ^{13}C NMR spectroscopy and gel permeation chromatography (GPC) techniques. The physico-chemical and physico-mechanical properties were tested by standard protocols. Initial decomposition temperature was measured by thermogravimetric analysis (TGA). The curing study and glass transition temperature were assessed by differential scanning calorimetry (DSC). Hydrophobicity of the coatings was measured in terms of contact angle. The anticorrosion performance of SA-BMF was studied experimentally using polarization techniques and electrochemical impedance spectroscopy (EIS), while the antimicrobial efficacy of the same were tested against Gram positive bacterium *Staphylococcus aureus* (*S. aureus*) and Gram negative bacterium *Escherichia coli* (*E. coli*) by the agar diffusion method. Overall, our studies revealed that the waterborne SA-BMF coating exhibited higher scratch resistance, impact resistance (150 lb/in.), and bend tests (flexibility retentive 1/8 in.), along with good antibacterial activity and anticorrosive performance. These coatings also find safe usage up to 200 °C.

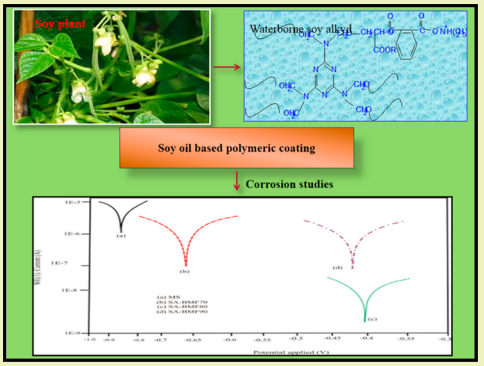

KEYWORDS: *Waterborne, Vegetable oil, Green solvent, Corrosion resistance, Antibacterial activity, EIS*

INTRODUCTION

The uncertainty about the cost of petroleum products, production of hazardous volatile organic compounds, and expected exhaustion of petroleum in the near future have raised the demand for the use of alternative materials and green technology, which is a perfect example of green chemistry "*a utilization of set of principles that help in the designing of hazard free products and processes*".[1−3] Furthermore, the introduction of new environmental legislations regarding the emission of volatile organic compounds (VOCs) have led to intensive research for the development of promising sustainable resource-based substitutes for petroleum products.[4] Among the various sustainable materials like lignin, cellulose,[5] starch, vegetable oil, etc.,[6] the vegetable oils are considered to be a potential alternative for petroleum feed stocks because of their low cost, environmental benignness in nature, reduced toxicity, low risk in transportation, multifunctionality, and physical and chemical stability.[7] The various oil-based low molecular weight polymers like polyesteramide,[8] polyetheramide,[9] polyurethane,[10] polyepoxy,[11] and alkyd[12] of various chain lengths have been reported. These polymers find wide applications in the manufacture of ink, adhesive, filler, paints, and coatings.[7] However, oil-based polymers fail to give good strength, alkaline resistance, stiffness, and rigidity for industrial applications. Hence, there is a need to modify oil-based polymers to obtain reasonably useful materials that find applications in various industries like ink, lubricants, adhesives, paints, and coatings.[13]

Alkyd resins are oil-modified polyesters, which are widely used in the surface coating industries and have shown great potential in coating applications.[14,15] Alkyd resins possess several advantages like excellent gloss, solvent resistance, and low cost and because of these they have attained a unique position in the coating industry.[12] However, traditionally alkyd resins involve the use of organic solvents, which significantly produce VOCs responsible for increased human health risks. For this reason, waterborne alkyds have received much attention due to their low or zero VOCs.[16] Alkyds are made waterborne by the introduction of carboxyl groups.[17] Nonetheless, waterborne alkyd coatings show slow drying and tackiness. Therefore, they are usually stoved with melamine formaldehyde or urea formaldehyde resin.[18] Moreover, their uses are restricted to general applications due to their poor acid, water, and alkali resistance.[19] Hence, the modification of alkyd resins to improve desired properties and avoid solvents

Received: April 14, 2013
Revised: July 16, 2013
Published: July 26, 2013

   dx.doi.org/10.1021/sc4001077 | ACS Sustainable Chem. Eng. 2013, 1, 1246−1257

producing VOCs has been a subject of intensive research. The modification of alkyd with a moiety containing the s-triazine unit has found to have a pronounced effect on physico-mechanical, thermal,[20] antibacterial,[21] and anticorrosive properties.

In recent years, synthesis of antibacterial polymers has been a topic of research for the development of promising antibacterial coating materials, to find applications for preventing the bacterial contamination in food, medical implants, and devices because they show better efficacy, reduced toxicity, increased selectivity, and prolonged stability. Hence, we have also investigated antibacterial activity in addition to anticorrosive performance of the coating.[21−23] There are large numbers of reports available on the antibacterial and anticorrosive behavior of solvent borne and waterborne polymers with different moieties as discussed in the following paragraph.

Polyetheramide-butylated melamine formaldehyde-based anticorrosive coating from renewable resources has been reported by Ahmad et al.[12] Aigbodion et al.[24,25] have developed maleinized and fumarised rubber seed oil alkyds for their use in waterborne coatings. Saravari et al.[12] have prepared maleic anhydride and n-butyl methacrylate copolymer-modified palm oil-based waterborne alkyd with improved water, acid, and alkali resistance using the chemical resistance method. Dhoke et al. synthesized anticorrosive coating material using commercial alkyd and characterized their anticorrosive performance by salt mist and chemical resistance method.[26] Literature[24−26] surveys reveal that the effect of a s-triazine ring on antibacterial and anticorrosive studies of waterborne soy alkyd has not been reported to the best of our knowledge. Therefore, in this study, we have reported the synthesis, characterization, antibacterial activity, and anticorrosive performance of waterborne soy alkyd modified with BMF. The structural analysis was carried out by spectroscopic techniques. Physico-chemical and physico-mechanical properties were evaluated by standard methods. Molecular weight of the polymer was determined using gel permeation chromatography (GPC). The effect of BMF loading on thermal stability, glass transition, antibacterial, and anticorrosive behavior was also evaluated. The unique combinations of soy oil and the s-triazine unit introduce hydrophobic characteristics giving a complete moisture barrier and further prevent the diffusion of electrolytes. These features make resins more interesting and find potential scope in packaging, paint, and coating applications.

EXPERIMENTAL SECTION

Materials. Soybean oil and butylated melamine formaldehyde (BMF) were received from Shanker Dyes & Chemicals (New Delhi, India) and phthalic anhydride (98%) from SD Fine Chemicals (Mumbai, India). Sodium hydroxide (97%), sodium chloride (99%), triethylamine (99%), glycerol (98%), and hydrochloric acid (35−36%) were obtained from Fisher Scientific (New Delhi, India). All the reagents were used as such without further purification.

Synthesis of Soy Monoglyceride (SMG). Soy oil, glycerol, and sodium hydroxide in 1:2:0.01 molar ratios were charged in a three necked round-bottomed flask equipped with a nitrogen inlet tube, thermometer, and magnetic stirrer. The reaction was carried out at 180 °C for 1.5 h with continuous stirring. The progress of the reaction was monitored at regular intervals of time by measuring the extent of solubility of the reaction product in methanol and FT-IR spectra. The formation of SMG was confirmed by the solubility test using one part of the reaction product in three parts of methanol.[27]

Synthesis of Waterborne Soy Alkyd (SA). Waterborne SA was synthesized by the reaction of SMG with phthalic anhydride (PA) (1: 0.5 molar ratio) in a three necked round-bottomed flask equipped with a dean stark condenser, magnetic stirrer, and thermometer. The reaction mixture was heated to 190 °C for 1 h with continuous stirring. The progress of the reaction was monitored by acid value and FT-IR spectroscopy. The reaction was terminated on achieving the desired acid value (40 mg/KOH). The reaction product was cooled to 60 °C. Triethylamine (as neutralizing agent) was added to the reaction product followed by the addition of a water−methanol blend.[12]

Synthesis of BMF Cured Waterborne Soy Alkyd (SA-BMF). The above reaction set up (used for SA) was used to synthesize the BMF-modified alkyd resin using a reaction mixture of soy alkyd and various ratios of BMF in the presence of a green solvent, i.e., blend of (water−methanol) and paratoulene sulfonic acid as catalyst. The reaction was carried out at 120 °C for 30 min with continuous stirring. Scheme 1 represents the synthesis of BMF-modified waterborne soy alkyd. The resins are named SA-BMF70, SA-BMF80, SA-BMF90, where the suffixes are a percentage of BMF. The reaction takes place between the butoxy of BMF and hydroxyl group of alkyd,[28] which resulted in the formation of a three-dimensional thermoset with the release of alcohol (Scheme 2).[29]

Characterization and Testing. FT-IR spectra of soy alkyd and SA-BMF were recorded on IR Affinity-1 Shimadzu using a ZnSe cell. ^{1}H NMR and ^{13}C NMR spectra of these resins were obtained on a JEOL GSX 300 MHz FX-100 in $CDCl_3$ using TMS as the internal standard. Molecular weights of the same were determined usinga Hitachi ELITE LaChrom chromatograph. Tetrahydrofuran (THF) was used as solvent and polystyrene as the standard.

The acid value, hydroxyl value, specific gravity, refractive index, and solubility as physico-chemical properties of the resins were measured using standard methods.[30] The mild steel specimens were polished successively with fine grade emery papers (600−800 grade). The specimens were washed thoroughly with double distilled water, degreased with ethanol and acetone, and dried at room temperature. Different ratios of SA-BMF were applied by a brush technique on commercial available mild steel strips (MS) of standard size MS, i.e., (70 mm × 25 mm × 1 mm) for a physico-mechanical test and (25 mm × 25 mm × 1 mm) for an electrochemical corrosion test. The scratch hardness (SH) [BS 3900], impact resistance (IRt) [IS; 101 part 5/sec-3, 1998], bending test (BT) [ASTM-D3281-84], specular gloss (at 45°), cross-hatch test [ASTM D3359], and methyl ethyl ketone (MEK) solvent resistance test [ASTM D5402] resin were measured for evaluation of physico-mechanical properties of the coating. The gel content of the coating material was done to evaluate the degree of cross-linking.[31] Contact angles were recorded on a Drop Shape Analysis System, model DSA10MK2 from Krüss GmbH, Germany.

Thermo-gravimetric analysis (TGA/DTA) of the cured resin was carried out on a EXSTAR TG/DTA 6000 under nitrogen atmosphere at a heating rate of 20 °C min^{-1}. Differential scanning calorimetry SII EXSTAR 6000, DSC620, Japan, was used to study the curing and glass transition behavior of SA-BMF resin mixture at a heating rate of 10 °C/min under nitrogen atmosphere.

The antibacterial behavior of SA and all the compositions of SA-BMF were investigated against *S. aureus* (Gram positive) and *E. coli* (Gram negative) bacteria using the agar diffusion method.[32] One loopful of bacteria was inoculated in 10 mL of nutrient broth (peptone 5gL, pH 6.8) and incubated at 37 °C for 28−30 h in a test tube shaker at 100 rpm. The actively growing bacterial cells were used for inhibition studies. The nutrient agar (20 mL) was poured into sterile Petri dishes and allowed to solidify at room temperature. After solidification, 0.1 mL of the bacterial culture was spread on the nutrient agar. A circular well (9 mm, diameter) was made with a sterilized steel borer, and 10 μL of each test solutions were added into the well and incubated at 37 °C for 24 h. The extent of the diameter (area) of inhibition zone around the well can be attributed to the promising antibacterial activity of the SA-BMF resin.

Electrochemical experiments of coated and uncoated mild steel strip (MS) were conducted in a conventional three electrode EG&G flat glass cell of capacity 400 mL using a potentiodynamic/galvanostat micro Autolab type III (μ 3AVT 70762, The Netherlands) in 3.5 wt % of HCl, 3.5 wt % of NaOH solutions, and tap water (Cl^- ion 63 mg/L; conductivity 0.953 mS/A) at room temperature (30 °C). Laboratory

Scheme 1. Synthesis of BMF-Modified Waterborne Soy Alkyd

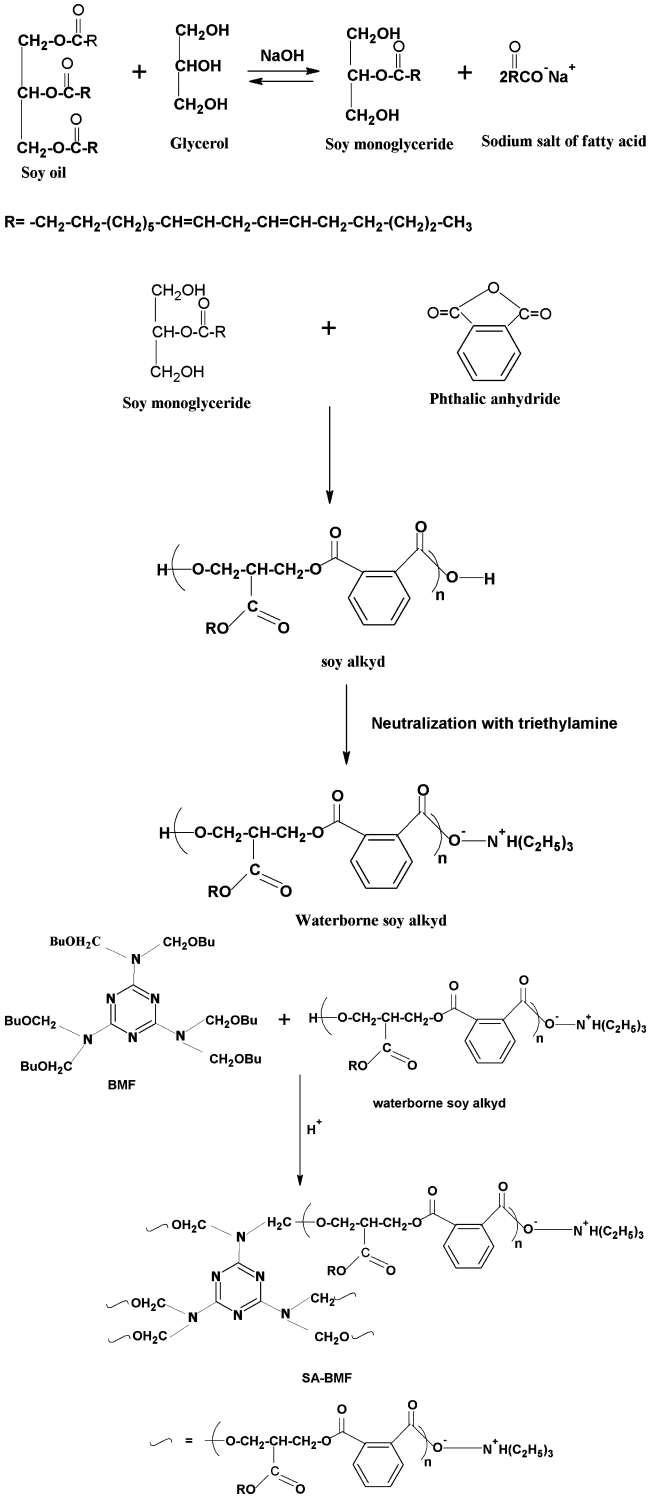

tap water contains Cl^- ion 63 mg/L (conductivity 0.953 mS/A) at room temperature. Chloride ions are highly effective corrosion initiators, which initiate pitting because of their small and highly mobile nature.[33] Hence, the corrosion protective performance of SA-BMF coating in tap water was carried out using the PDP and EIS technique.

The three electrodes are Ag/AgCl as reference, platinum as auxiliary, and test specimen as the working electrode. A total of 1.0 cm^2 area of working electrode was exposed to the solution.

Before the electrochemical test, the working electrode was allowed to stabilize for 20 min, and then its OCP was recorded as a function of time for 600 s. After OCP stabilization, impedance measurements were made at respective corrosion potentials (E_{corr}) over a frequency range of 100 kHz−0.1 Hz, with a signal amplitude perturbation of 10 mV. Potentiodynamic polarization studies were carried out in the potential range of ±100 mV (with respect to OCP) at 0.001 mV/s scan rate. Nova 1.8 softwares were used for data fitting and calculation of results. The impedance and Tafel parameters were extracted by curve fitting procedures available in the software. Each test was run in triplicate to verify the reproducibility of the data.

RESULTS AND DISCUSSION

Characterization of Synthesized Resin. Figure 1 represents the FT-IR spectra of SMG, waterborne SA, and SA-BMF90. The band at 3410 cm^{-1} corresponded to the hydroxyl group in monoglyceride (Figure 1a), and the same band appears with lower intensity in waterborne soy alkyd and SA-BMF resin (Figure 1b,c). The FT-IR spectra of soy alkyd resin (Figure 1b) exhibited a band at 1726 cm^{-1} for ester linkages.[8] The bands at 2932 cm^{-1} and 2891 cm^{-1} can be ascribed to the −C−H asymmetric and symmetric stretching absorptions of the $-CH_3$ and $-CH_2$ groups of fatty acid present in alkyd.[34] In addition, the band at 1655 cm^{-1} has been assigned to −CH═CH stretching vibration of double bond. The presence of a characteristic band at 1596 cm^{-1} is evidence for the transformation of a terminal carboxylic group to a carboxylate anion.[10] Besides, the band at 962 cm^{-1} is due to the $-COO-N^+H(C_2H_5)_3$ stretching vibration, indicating that the tertiary nitrogen atoms got converted to the quaternary ammonium moiety.[35] The above-mentioned bands revealed the formation of waterborne soy alkyd through the reaction of an acid group of phthalic anhydride with hydroxyl groups of soy monoglyceride. In Figure 1c, the band at 1552 cm^{-1} is attributed to the plane stretching of a s-triazine ring of BMF introduced in SA. An additional band also occurred at 1036−1073 cm^{-1}, which further confirmed the etherification reaction of SA with BMF moiety.[30]

In Figure 2a, the peak at δ = 0.94−0.99 ppm was assigned to the terminal methyl group of a fatty acid chain.[35] The peak for protons attached directly to the terminal methyl group appeared at δ = 1.2−1.59 ppm, while the peak at δ =1.25−1.29 ppm can be ascribed to the protons of all the internal $-CH_2-$ groups present in the fatty acid chains.[25] The peak at δ = 5.5 ppm was due to the protons attached to the unsaturated carbon of fatty acid chain. The peak at δ = 7.3−7.5 ppm was assigned to the aromatic protons of phthalic anhydride present in alkyd.[36] In addition, the signal at δ = 4.4−4.6 ppm corresponded to the $-CH_2-O-C{=}O$ proton present in the backbone of the waterborne soy alkyd.[17] ^{1}H NMR spectra of SA-BMF (Figure 2b) exhibited a peak at δ = 3.2−3.8 ppm and appeared as a tall peak for $(-OCH_2)$,[3037] formed by the etherification reaction of SA with BMF, leading to the formation of SA-BMF resin. The peaks from different fragments severely overlap and make their direct assignment impossible.

Figure 2c shows the ^{13}C NMR spectrum of SA. The peaks at δ =173 ppm and at δ =129−131 ppm corresponded to the carbonyl carbon of ester linkage and aromatic carbons of phthalic anhydride. Besides, the peak in the region of δ = 30−70 ppm was assigned to the carbon atom directly attached to an oxygen atom. The peaks at δ = 0−35 ppm and at δ = 127 ppm corresponded to methyl, methylene carbon, and olefinic carbon of a fatty acid chain.[23] Along with the above-mentioned peaks,

Scheme 2. Curing of Waterborne Soy Alkyd with BMF

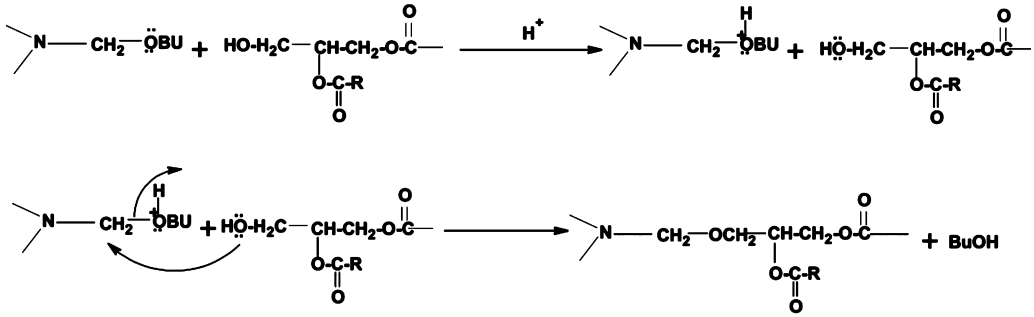

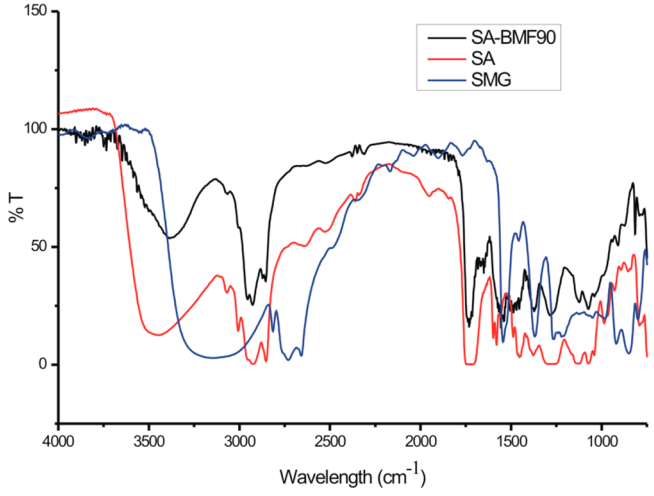

Figure 1. FT-IR spectra of SMG, SA, and SA-BMF.

the ^{13}C NMR spectra of SA-BMF (Figure 2d) showed a peak around δ = 170 ppm that corresponds to the carbon atoms of the symmetrical triazine ring,[38] confirming the reaction of BMF with soy alkyd.

Physico-Chemical Characteristics of SMG, SA, and SA-BMF. Table S1 (Supporting Information) depicts the physico-chemical properties of the synthesized resin. It is shown that there was a gradual increase in specific gravity and refractive index values from SMG, SA, to SA-BMF, which can be attributed to the inclusion of a BMF ring in alkyd. The formation of SA by the reaction of SMG and phthalic anhydride was also confirmed by the drop in acid value during the progress of the reaction. Hydroxyl values decreased from SMG to SA-BMF, attributed to the consumption of hydroxyl groups through the chemical reaction between hydroxyl groups of SMG and the carboxyl group phthalic anhydride, later between hydroxyls of SA and butoxy groups of BMF. The solubility of SMG, waterborne SA, and SA-BMF were tested in polar and nonpolar solvents. The results are summarized in Table S2 (Supporting Information). The SMG was soluble in tetrahydrofuran (THF), toluene, hexane, and xylene but partially soluble in dimethyl sulphoxide (DMSO) and dimethylformamide (DMF), while SA and SA-BMF were found to be completely soluble in DMSO, DMF, THF, and a water:-methanol blend (70:30) but insoluble in nonpolar solvents. From the solubility test, it was found that the SA and SA-BMF were soluble in highly polar solvents like DMSO and DMF but insoluble in nonpolar solvents. This may be due to the presence of a salt structure (COO^- NH^+ $(C_2H_5)_3$, polar −NH groups, or rigid triazine units of BMF present in SA and SA-BMF.[39]

Physico-Mechanical and Gel Content Properties of SA-BMF Coatings. The physico-mechanical properties of SA-BMF70, SA-BMF80, and SA-BMF90 are given in Table 1. The drying time decreased and gloss value increased with increasing the content of BMF in waterborne soy alkyd. The increase in gloss value from SMG to SA-BMF90 can be attributed to the increase in the cross-linking network due to which a large amount of light was reflected from the coating surface.[40] An improvement was observed in scratch hardness values from SA-BMF70 to SA-BMF90. This can be explained by the formation of an effective network after inclusion of a BMF ring in soy alkyd, which restricts the indentation,[40] and also an increase in adhesion between SA-BMF and a metal substrate.[41] Furthermore, an increase in adhesion of a SA-BMF coating with the metal surface was confirmed by a cross hatch test. As the content of BMF increased from 70 Phr (per hundred ratio) to 90 Phr, the coating surfaces were found to smoothen with no peeling.[42] All the coatings were found to pass the impact resistance test as SA-BMF contained flexible moieties like ether linkages as well as long hydrocarbon chains of soy oil, which can dissipate the impact energy by segmental motion in their molecular chains.[43] Likewise, coatings were also found to pass the conical bend tests from SA-BMF70 to SA-BMF90. The flexibility of the coatings were due to the presence of an oil aliphatic moiety and ether linkages present in the resin structure that offers the plasticizing effect in the coating.[43] The gel content of the coating was also determined for the quantification of the degree of cross-linking as the degree of cross-linking is directly related to the extent of gel content. The value of gel content increased with an increase in the BMF amount in soy alkyd (i.e., SA-BMF70 < SA-BMF80 < SA-BMF90), which suggested an increase in the formation of a highly cross-linked network.

The contact angle images of coatings as a function of BMF content (Figure 3) revealed that the incorporation of BMF into waterborne alkyd significantly enhanced the value of the contact angle from 83° to 95°. This can be due to the presence of a rigid cross-linker (BMF), which resulted in an increase in the hydrophobic character of the coatings with low wet ability. This acts as an efficient barrier layer to impede the diffusion of electrolytes inducing good corrosion resistance properties,[44] which is also evident from the low corrosion rate values of the coatings.

Gel Permeation Chromatography (GPC). The number average (M_n), weight average molecular weight (M_w), and polydispersity index (PI) for SA, SA-BMF70, SA-BMF80, and SA-BMF90 were determined by gel permeation chromatography, given in Table 2. The values for M_n, M_w, and PI gradually

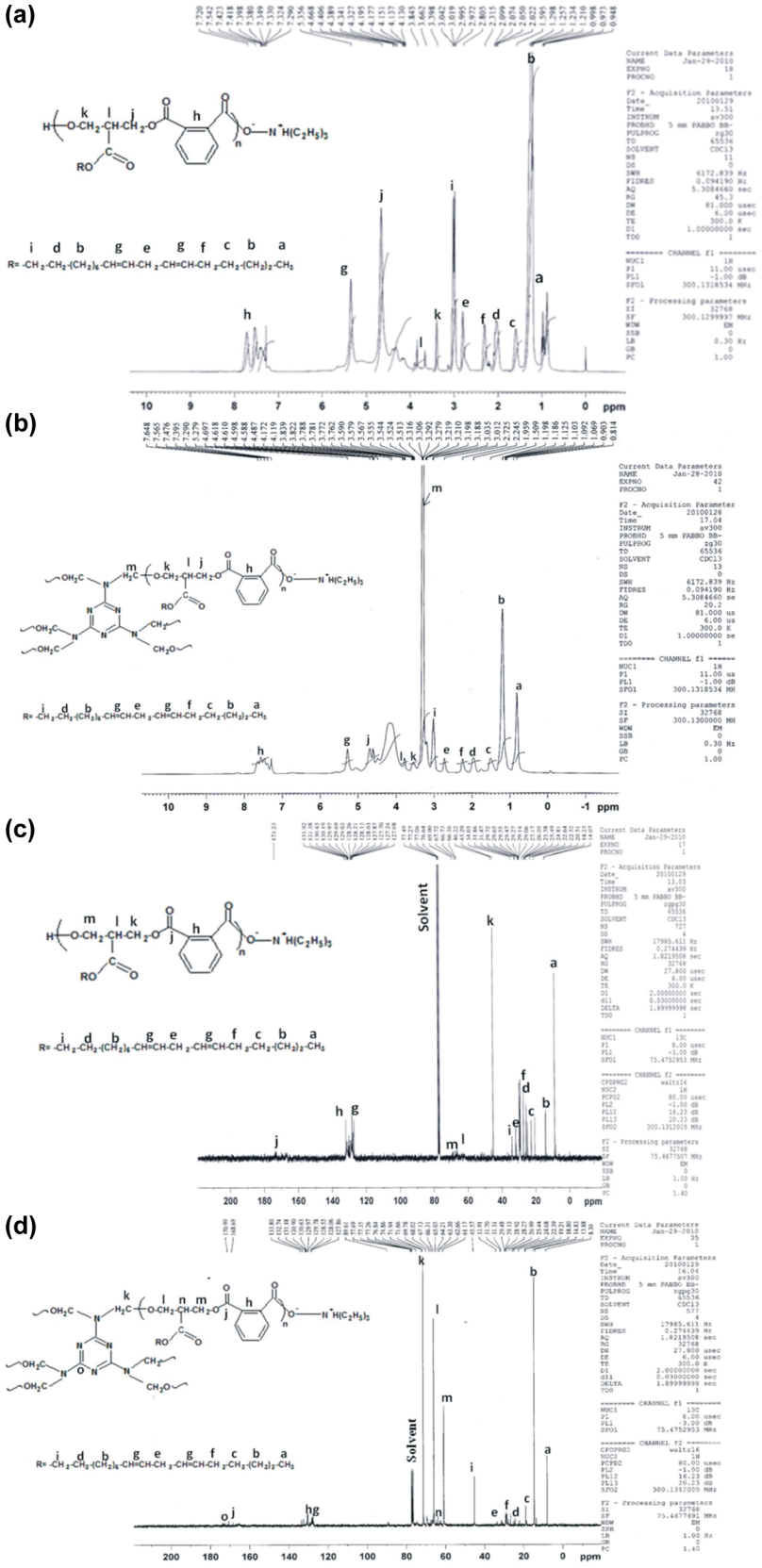

Figure 2. (a) ^{1}H NMR spectra of SA. (b) ^{1}H NMR spectra of SA-BMF. (c) ^{13}C NMR spectra of SA. (d) ^{13}C NMR spectra of SA-BMF.

increased with an increase in BMF content due to the formation of effective cross-link density.

Glass Transition and Curing Behavior of SA-BMF Resins. In order to obtain good coating properties, it is necessary to optimize the curing conditions. Figure 4 shows the curing curves obtained by dynamic DSC for the curing of SA-BMF, both in the presence and absence of a catalyst. To confirm complete curing behavior of the resin, samples after the

dx.doi.org/10.1021/sc4001077 | ACS Sustainable Chem. Eng. 2013, 1, 1246−1257

Table 1. Physico-Mechanical Test of All Compositions of SA-BMF oating

resin code	SA-BMF70	SA-BMF80	SA-BMF90
gloss (45°)	39	45	50
scratch hardness (kg)	4	5	5.8
impact resistance (150 lb/inch)	pass	pass	pass
bending (1/8 in.)	pass	pass	pass
drying time (min)	30	20	15
cross hatch test	fail	pass	pass
MEK	>500	>500	>500

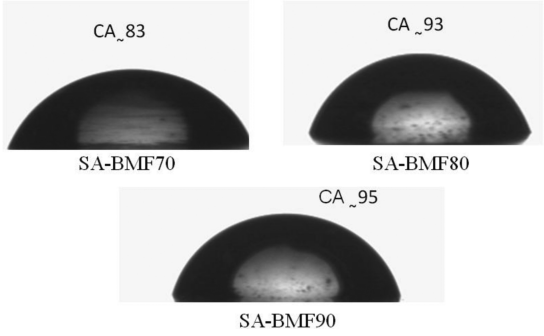

Figure 3. Contact images of different ratio of SA-BMF.

Table 2. Molecular Weight of SA and Modified Soy Alkyd Resin (SA-BMF)

resin code	M_n	M_w	PI
S-Alk	2603	3615	1.38
SA-BMF70	3204	6828	2.13
SA-BMF80	3485	7964	2.28
SA-BMF90	3698	10450	2.82

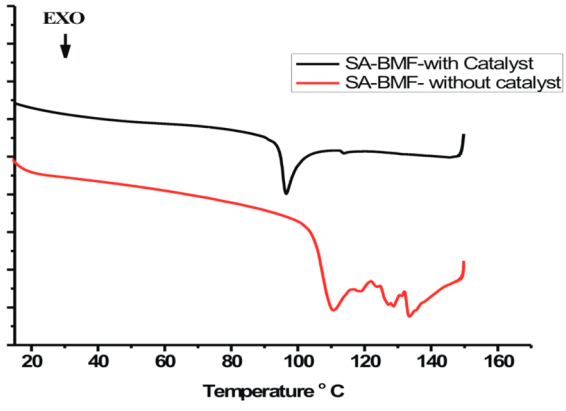

Figure 4. Curing study of SA-BMF mixture.

first scan were cooled, and then the cooled samples were again rescanned from 10 to 200 °C at a heating rate of 10 °C/min. There were no more noticeable peaks observed in second scan heating. In Figure 4, a sharp exothermic peak appeared at around 95 °C, which may be regarded as the onset of the cure reaction for soy alkyd and BMF resin,[45] and the maximum is attained around 118 °C in the presence of the catalyst. However, in the absence of a catalyst, the onset of the broad exothermic peak appeared at around 110 °C (Figure 4), indicating the partial cross-linking reaction between alkyd and melamine resin, and the peak endset is attained around 135 °C. The DSC results also revealed that the sharp exothermic peak

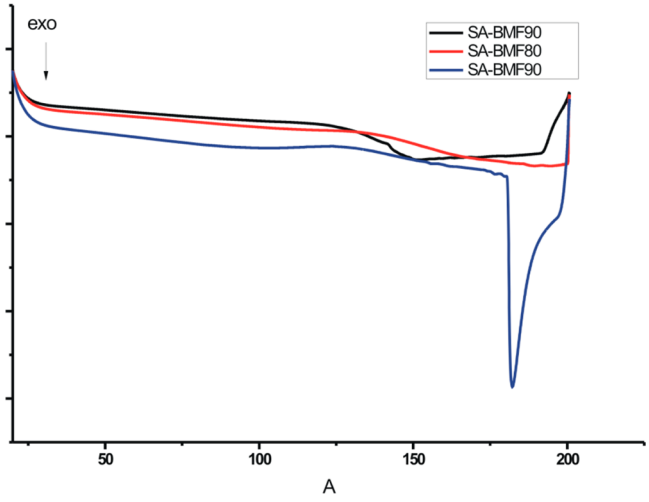

Figure 5. DSC curves of different ratios of SA-BMF.

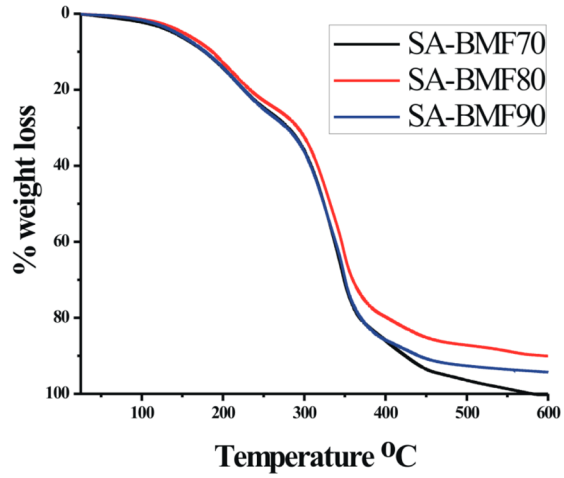

Figure 6. Weight loss curves of different ratios of SA-BMF resin by TGA.

Table 3. Inhibition Zone on Agar Plate after Incubation of Bacteria with Different Amounts of BMF in Soy Alkyd[a]

species	SA-BMF70	SA-BMF80	SA-BMF90
E. coli	++	++	++
S.aureus	+++	+++	++++

[a] ++ Mildly active (3−5 mm). +++Moderately active (8−10 mm). +++ +Moderate to slightly high active (10−15 mm).

at low temperature in the presence of a catalyst indicates a better cross-linking reaction in comparison to that of without a catalyst.[29] Keeping these facts in mind, we had carried out the reaction in the presence of a catalyst to obtain better cross-linking.

The T_g curves for different ratios of SA-BMF polymers are given in Figure 5. The glass transition temperature was found to be in the range of 110−145 °C. The increase in T_g values from SA-BMF70 to SA-BMF90 (SA-BMF70 = 120 °C, SA-BMF80 = 135 °C, SA-BMF90 = 145 °C) was due to presence of a high content of melamine ring, which resulted in the formation of highly cross-linked network.[46]

Thermal Properties. The thermal degradation behavior of BMF-modified waterborne soy alkyd is shown in Figure 6. The 5 wt % loss occurred in the range of 100−120 °C, attributed to

dx.doi.org/10.1021/sc4001077 | ACS Sustainable Chem. Eng. 2013, 1, 1246−1257

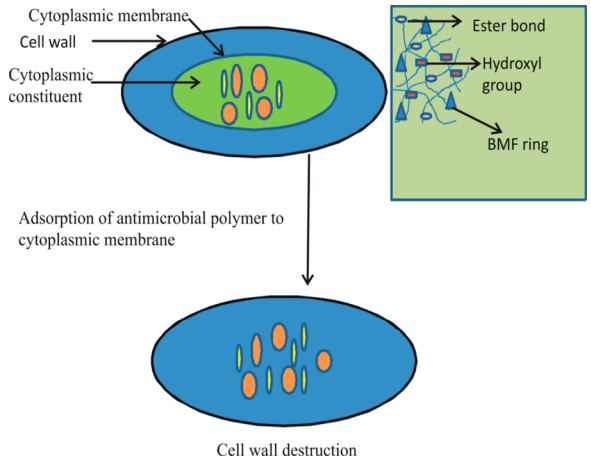

Figure 7. Probable mechanism of antibacterial activity of SA-BMF.

the release of trapped solvent molecules in SA-BMF network. SA-BMF polymers were degraded bya two-step process, where the first step was related to the de-cross-linking between SA and BMF[47] (190−200 °C), followed by the second step of degradation (290−300 °C) of ester, ether, and melamine ring.[48] All SA-BMF polymers have the same structural units,and their degradation pattern and degradation temperature were almost same with a slightly higher degradation temperature in SA-BMF80. The low thermal stability of SA-BMF90 in comparison to SA-BMF80, though the former contains a higher amount of BMF ring, may be due to high degree of cross-link network,[30] resulting in the formation of a strained structure, which causes steric hindrance to the free rotation of shorter polyether links and introduced rigidity in the system.

Antibacterial Activity. Antibacterial activities of SA and different ratios of SA-BMF were carried out against *E. coli* and *S. aureus* with the agar diffusion method. Table 3 shows the size (diameter, mm) of inhibition zones on agar plates after incubation of bacteria with different amounts of BMF in soy alkyd. To confirm that the antibacterial activities were mainly derived from the BMF moiety, control experiments were carried out in which neat waterborne SA was used. When the antibacterial experiment was carried out on SA against *E. coli* and *S. aureus*, an insignificant inhibition zone was observed, indicating negligible antibacterial activities of SA against both bacterial strains. Although plain waterborne alkyd possesses a quaternary nitrogen atom formed by neutralizing carboxyl groups with triethylamine, which is likely to induce satisfactory antibacterial activity. The insignificant inhibition zone of SA might be due to the hydrophobic part (soy oil) present in the alkyd, which may result in partial aggregation within the culture medium and decreased antibacterial action. As a result, less interaction occurred between the polymer and bacteria.[22] SA-BMF resin exhibits good antibacterial activity against both *S. aureus* and *E. coli*, though slightly better against *S. aureus*. Besides, 1, 3, and 5 s-triazine-based derivatives prefentially kill Gram positive bacteria as compared to Gram negative bacteria.[49] The difference in activity for *S. aureus* and *E. coli* can be due to the difference in the structure and composition of their cell wall. In *S. aureus*, the SA-BMF polymer might interact more effectively with the cell wall of Gram positive bacteria, where the polyglycogen outer layer is sufficiently loosely packed to facilate the deep penetration of the polymer. On the other hand, the cell wall of Gram negative bacteria is overlaid with an additional outer membrane with a bilayer phospholipids

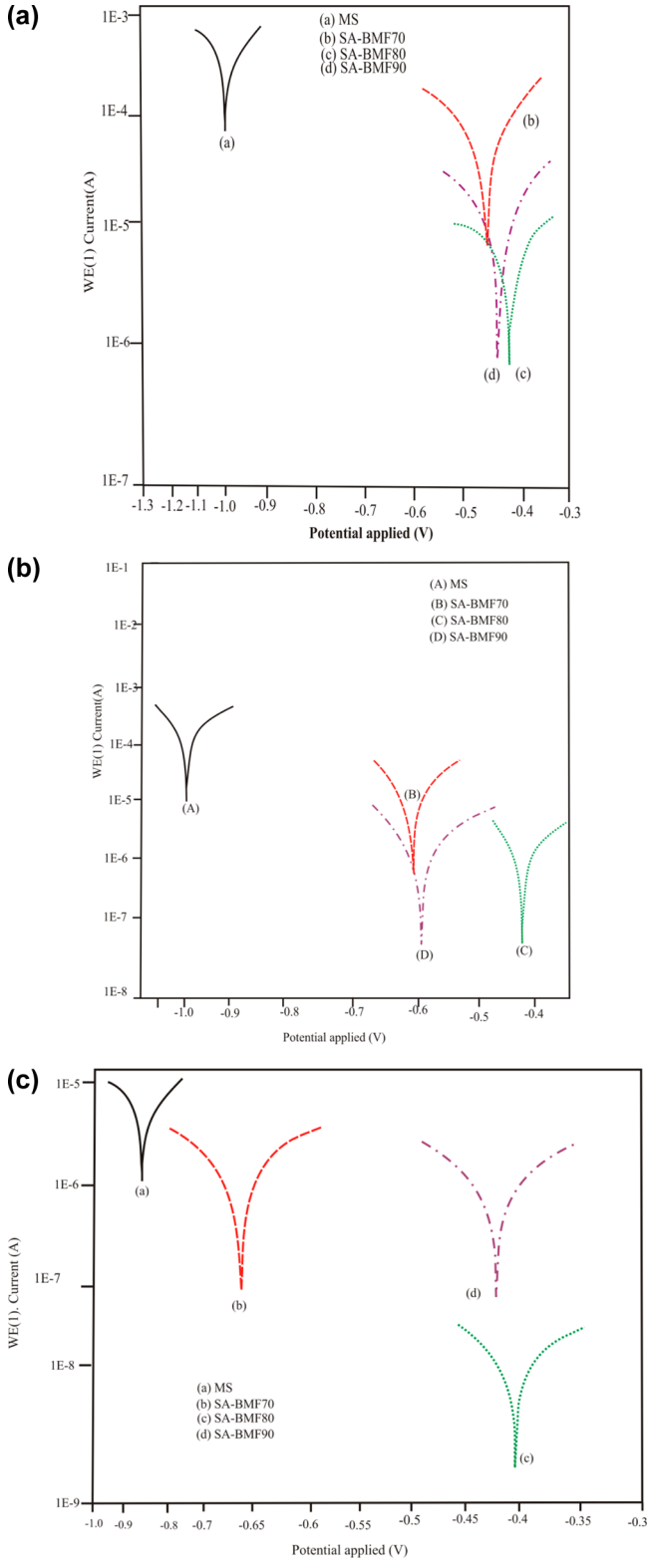

Figure 8. (a) Potentiodynamic polarization of coated and uncoated MS in 3.5 wt % HCl. (b) Potentiodynamic polarization of coated and uncoated MS in 3.5 wt % NaOH. (c) Potentiodynamic polarization of coated and uncoated MS in tap water.

structure, which offers a supplementary barrier and prevens the penetration of a wide range of antimicrobial agents into the cell.[21]

Table 4. Corrosion Parameters for SA-BMF-Coated and -Uncoated Mild Steel Strips in Different Corrosive Environments

resin	medium	E_{corr} (V)	I_{corr} (Å/cm^2)	polarization resistance (ohm)	corrosion rate (mpy)
MS	3.5% HCl	−1.020	2.45×10^{-4}	808.62	0.3280
SA-BMF70	3.5% HCl	−0.460	2.82×10^{-5}	1.13×10^{3}	0.0528
SA-BMF80	3.5% HCl	−0.444	1.44×10^{-6}	5.56×10^{3}	0.0167
SA-BMF90	3.5% HCl	−0.451	3.16×10^{-6}	4.42×10^{3}	0.0367
MS	3.5% NaOH	−1.080	1.67×10^{-5}	993.43	0.1941
SA-BMF70	3.5% NaOH	−0.596	4.15×10^{-6}	1.45×10^{4}	0.0482
SA-BMF80	3.5% NaOH	−0.425	2.17×10^{-7}	1.67×10^{5}	0.0020
SA-BMF90	3.5% NaOH	−0.593	2.34×10^{-7}	1.64×10^{5}	0.0027
MS	Tap water	−0.868	7.23×10^{-6}	498.02	0.3162
SA-BMF70	Tap water	−0.642	4.35×10^{-7}	8.30×10^{4}	0.0058
SA-BMF80	tap water	−0.405	3.22×10^{-9}	2.17×10^{7}	0.0024
SA-BMF90	tap water	−0.416	1.93×10^{-7}	2.74×10^{4}	0.0050

Table 5. Electrochemical Impedance Parameters for Uncoated SA-BMF and Coated MS in Different Corrosives at Room Temperature

resin	medium	R_{pore}(ohm)	C_c (farad)	n
MS	3.5% HCl	21		
SA-BMF70	3.5% HCl	5.32×10^{4}	4.29×10^{-5}	0.748
SA-BMF80	3.5% HCl	3.35×10^{5}	3.26×10^{-6}	0.477
SA-BMF90	3.5% HCl	7.64×10^{4}	5.85×10^{-6}	0.594
MS	3.5% NaOH	27.5		
SA-BMF70	3.5% NaOH	2.75×10^{4}	1.22×10^{-5}	0.799
SA-BMF80	3.5% NaOH	4.98×10^{5}	1.78×10^{-6}	0.577
SA-BMF90	3.5% NaOH	3.33×10^{5}	9.67×10^{-6}	0.670
MS	tap water	35	-	
SA-BMF70	tap water	3.40×10^{5}	2.69×10^{-6}	0.659
SA-BMF80	tap water	3.03×10^{7}	2.21×10^{-9}	0.537
SA-BMF90	tap water	5.03×10^{5}	8.04×10^{-7}	0.546

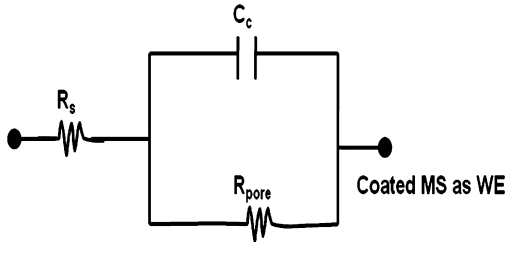

Figure 9. EIS circuit.

The effect of molecular weight on antibacterial activity was also investigated. This study indicates that polymers with molecular weight up to 5×10^4 to 9×10^4 Da do not have any problems in diffusing across the cell wall of the Gram positive bacterium (*S. aureus*). The molecular weight of SA-BMF polymer (GPC results, Table 2) is in good agreement with the literature value. For Gram negative bacteria (*E. coli*), the question of diffusion to the cell membrane is more complicated because of the existence of an additional membrane.[23] Figure 7 illustrates the probable mechanism of the antibacterial activity of the SA-BMF polymer, although a detailed mechanism of antibacterial action of SA-BMF was not extensively investigated in this study. The antibacterial activity of the SA-BMF resin could be attributed to the presence of an ester bond present in the polymer backbone that can possibly be hydrolyzed to give a small antibacterial molecules.[50] Besides, hydrogen bonding might have occurred between the residual hydroxyl group with the phosphate, carbonyl, or hydroxyl oxygen atoms of the molecules of phospholipids, polysaccharides, or teichoic acid embedded in the membrane of the Gram positive cell wall thus causing lateral segregation of negatively charged lipids and permeability of the outer membrane.[51]

Potentiodynamic Polarization (PDP) Studies. Figure 8 and Table 4 show the potentiodynamic polarization measurements for different ratios of SA-BMF-coated samples in different corrosive media (3.5 wt % HCl, 3.5 wt % NaOH, and tap water). Corrosion potential and corrosion current density were obtained by the extrapolation method, where anodic and cathodic curves were extrapolated to their point of intersections. The polarization resistance R_p was evaluated from Tafel plots, according to the Stearn−Geary equation

$$R_p = \frac{b_a b_c}{2.3(b_a + b_c) I_{corr}} \quad (1)$$

where b_a and b_c are anodic and cathodic Tafel slopes, respectively.[52] In 3.5 wt % HCl medium (Figure 8a), it was observed that SA-BMF80-coated MS had an E_{corr} value of −0.444 V, which was significantly toward the more positive direction in comparison to bare MS (E_{corr} −1.020 V). Similarly, its I_{corr} value decreased from 2.45×10^{-4} to 1.44×10^{-6} Å cm^{-2}. With respect to the bare MS, the polarization resistance value also increased for coated samples from 808.62 to 5.56×10^3 Ω. These results indicate that the SA-BMF-coated MS block the diffusion of electrolytes. Overall, the SA-BMF coated sample showed higher corrosion resistance performance than that of bare MS, which was further confirmed by the corrosion rate of these coatings (Table 4). The corrosion protection exhibited by SA-BMF polymers can be attributed to the presence of s-triazine rings, which inhibit the corrosion by blocking both anodic and cathodic sites in the HCl medium. In acidic solution, the s-triazine ring gets protonated and adsorbed on cathodic sites, decreasing the hydrogen evolution.[53] In the present study, the order of corrosion inhibition was found as SA-BMF80 > SA-BMF90 > SA-BMF70, although the contact angle value increases from SA-BMF70 to SA-BMF90, which suggests an increase in hydrophobic character. The poor performance displayed by SA-BMF70 can be corroborated to the presence of some pores due to low cross-link density, while in SA-BMF90, it might be due to the formation of a highly cross-linked structure, which resulted in a strained structure.[26,54]

In 3.5 wt % NaOH solutions (Figure 8b), SA-BMF coatings having higher corrosion potential and lower corrosion current density as compared to bare MS. Improved corrosion resistance performance of SA-BMF-coated substrate can be attributed to the presence of a reasonably good cross-linked network, which is formed by the introduction of BMF in waterborne SA, and also due to the hydrophobic surface of the coatings as evident

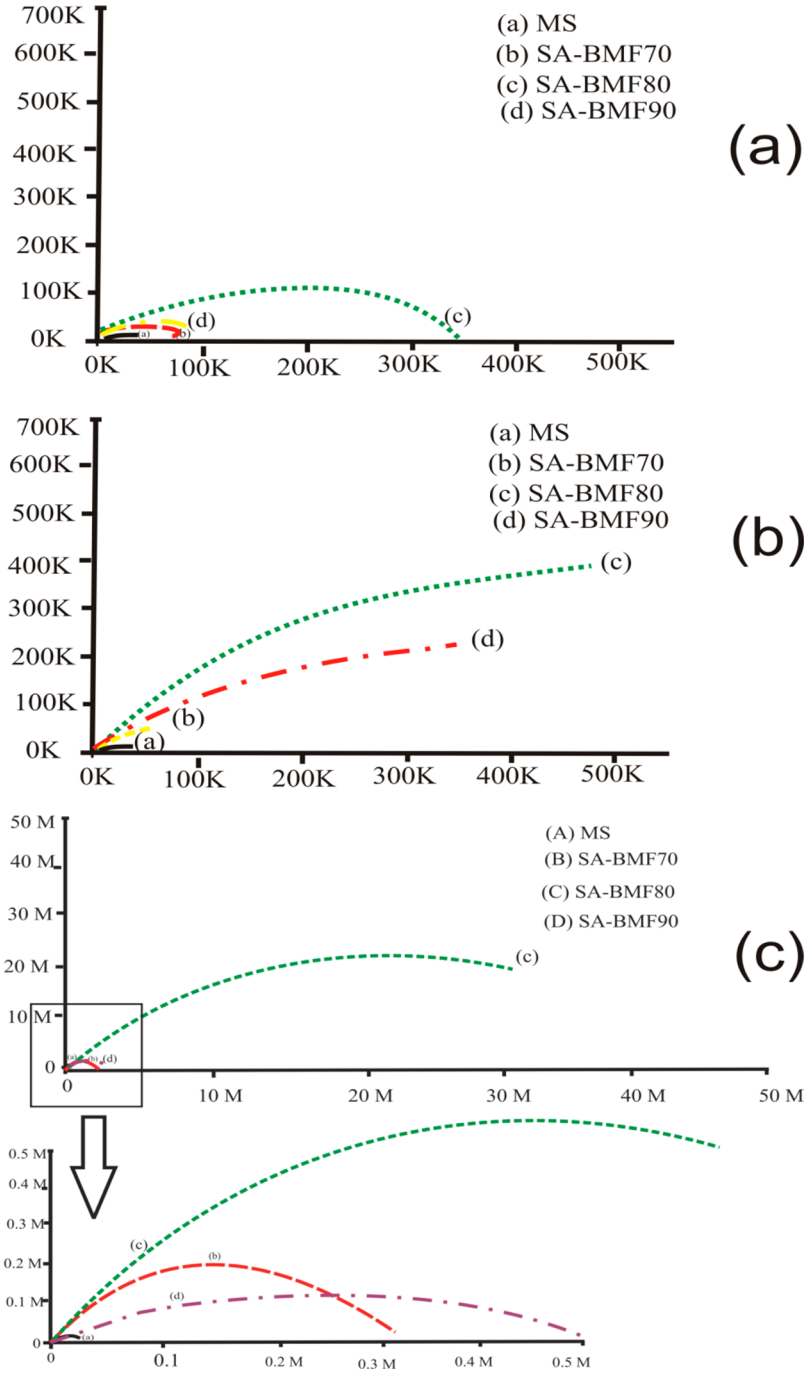

Figure 10. EIS study of SA-BMF coated and uncoated MS (a) 3.5 wt % HCl, (b) 3.5 wt % NaOH, and (c) tap water.

from the contact angle value. Hence, water molecules or any other corrosive ingredients do not penetrate through the surface of the coatings, which provide a good barrier property.[44,55] However, a shift toward low current density is more for SA-BMF80 as compared to SA-BMF70 and SA-BMF90. This can be attributed to the presence of micropores with low cross-linking density in SA-BMF70, while the highly cross-linked network is responsible for a strained structure in SA-BMF90.[53]

The presence of chloride ions in water being highly corrosive in nature causes corrosion of metal and alloys in contact with such water.[33] Hence, to see the effect of water containing the Cl^- ion on the protective ability of the coating materials (SA-BMF), the PDP and EIS studies in laboratory tap water (Cl^- ion 63 mg/L; conductivity 0.953 mS/A at room temperature of 30 °C) were carried out.

In tap water (Figure 8c), three coating,s namely, SA-BMF70, SA-BMF80, SA-BMF90, followed similar trends (SA-BMF80 > SA-BMF90 > SA-BMF70) as discussed above. The corrosion protection mechanism of SA-BMF coatings in tap water can be explained on the basis of the formation of a compact, uniform, impermeable, and hydrophobic layer at the interface of the metal substrate and tap water, which prohibits the permeation of ions through the coatings. This fact was further supported by shifting the E_{corr} value toward a noble direction for SA-BMF-coated MS as compared to uncoated MS.[55,56]

Electrochemical Impedance Spectroscopy (EIS) Studies. The SA-BMF coatings on MS were evaluated by

electrochemical impedance spectroscopy (EIS) in order to gain more insight into the anticorrosion behavior of these coatings. The electrochemical impedance spectra were recorded on uncoated MS and different compositions of SA-BMF coatings in 3.5 wt % HCl, 3.5 wt % NaOH, and tap water solutions. The results of the impedance measurements in different corrosive media are depicted in Table 5 and Figure 10.

Figure 9 gives the best fit equivalent circuit in different corrosive media, which includes solution resistance (R_s), pore resistance (R_{pore}), and coating capacitance (C_c). The high-frequency intercept is equal to the solution resistance, and the low-frequency intercept is equal to the sum of the solution and pore resistance.[57]

The 3.5% HCl medium (Figure 10a) shows the impedance behavior of coated and uncoated MS in the form of a Nyquist plot. Figure 10a reveals that the impedance spectra have depressed semicircles instead of perfect semicircles. Such phenomenon can be attributed to the surface heterogeneity and dislocation.[58] In comparison to bare MS, the pore resistance value increased from 21 to 3.33×10^5 in the case of SA-BMF-coated MS. The increase in the pore resistance value can be attributed to the formation of a protective film on the metal−solution interface. Furthermore, the coating capacitance value also reduced in the case of coated MS. The increase in R_{pore} and decrease in C_c indicates that SA-BMF-coated MS exhibit corrosion resistance behavior in acidic medium. The higher corrosion inhibition efficiency of BMF-modified soy alkyd could be attributed to the presence of π electrons, quaternary nitrogen atoms formed by the protonation in HCl medium, and planarity of the s-triazine ring.[53,59] In acid media, s-triazine rings get protonated, and these protonated rings are adsorbed on the cathodic sites of the metal and mask the evolution of hydrogen as described by Quraishi et al.[53,60] due to which the pore resistance value might get increased and the coating capacitance value decreased. However, among the different ratios of the coated samples, SA-BMF80 exhibited higher efficiency in comparison to SA-BMF70 and SA-BMF90. The poor performance displayed by SA-BMF90 in comparison to SA-BMF80 may be due to the reason discussed in the previous section. In 3.5% NaOH medium, Figure 10b shows that the higher pore resistance and lower coating capacitance value of SA-BMF80 as compared to bare MS suggests that the coated MS offer better corrosion protection by blocking the surface of MS through the reduction in oxygen and metal dissolution occurring within the pores of coating layers.[55,61] The high corrosion resistance performance of the coatings can be ascribed to the formation of a hydrophobic surface formed by the introduction of a BMF moiety that results in a highly cross-linked network through which moisture and other aggressive anions cannot penetrate easily and subsequently enhance the corrosion resistance performance of the coated metal surface. However, among the coated samples, SA-BMF80 exhibits a higher protective efficiency in comparison to SA-BMF70 and SA-BMF90 as discussed with the HCl medium.

In tap water (Figure 10c), the R_{pore} value was found to be at maximum, and C_c was found at the minimum for SA-BMF80-coated MS compared to that of bare MS. Here also the trend was the same among different coated samples, i.e., SA-BMF80 > SA-BMF90 > SA-BMF70. Corrosion protection offered by these coatings can be attributed to the formation of a highly cross-linked structure formed by the inclusion of BMF, which resulted in an efficient hydrophobic barrier layer to the electrolytes that can effectively separate the anode from cathode electrically.[44,62]

CONCLUSIONS

SA-BMF resin was successfully developed via a green route. The synthesized resins were characterized by different spectroscopic techniques. The incorporation of BMF induced antibacterial activity in SA, particularly against the Gram positive bacteria *S. aureus*. The antibacterial performance of the synthesized resin suggests their potential as a coating material in the food packaging industry. The contact angle, PDP, and EIS studies revealed good corrosion protection performance against acid, alkaline, and tap water media, which make them suitable for the surface coating industry.

ASSOCIATED CONTENT

Supporting Information

Tables S1 and S2 show the physico-chemical properties and solubility test of the synthesized resin. This material is available free of charge via the Internet at http://pubs.acs.org.

AUTHOR INFORMATION

Corresponding Author

*Tel.: +91 11 26827508. Fax: +91 11 26840229. E-mail: sharifahmad_jmi@yahoo.co.in.

Notes

The authors declare no competing financial interest.

ACKNOWLEDGMENTS

Shabnam Pathan is thankful for the financial support of the UGC-BSR meritorious fellowship No. F. 12006 (BSR/7-192/2007).

REFERENCES

(1) Uday, K.; Niranjan, K. Hyperbranched polyether core containing vegetable oil-modified polyester and its clay nanocomposites. *Polym. J.* **2011**, *43*, 565−576.

(2) Haq, M.; Burgueño, R.; Mohanty, A. K.; Misra, M. Hybrid bio-based composites from blends of unsaturated polyester and soybean oil reinforced with nanoclay and natural fibers. *Compos. Sci. Technol.* **2008**, *68*, 3344−3351.

(3) Sean, E.; Alex, M. C.; Antony, J. W. Incorporating green chemistry concepts into mobile chemistry applications and their potential uses. *ACS Sustainable Chem. Eng.* **2013**, *1*, 8−13.

(4) Raquez, J. M.; Deléglise, M.; Lacrampe, M. F.; Krawczak, P. Thermosetting biomaterials derived from renewable resources: a critical review. *Prog. Polym. Sci.* **2010**, *35*, 487−509.

(5) Yu, L.; Dean, K.; Li, L. Polymer blends and composites from renewable resources. *Prog. Polym. Sci.* **2006**, *31*, 576−602.

(6) Meier, M.; Metzger, J. O.; Schubert, U. S. Plant oil renewable resources as green alternatives in polymer science. *Chem. Soc. Rev.* **2007**, *36*, 1788−1802.

(7) Uyama, H.; Kuwabara, M.; Tsujimoto, T.; Nakano, M.; Usuki, A.; Kobayashi, S. Green nanocomposite from renewable resources: Plant oil−clay hybrid materials. *Chem. Mater.* **2003**, *15*, 2492−2494.

(8) Pramanik, S.; Konwarh, R.; Sagar, K.; Konwar, B. K.; Karak, N. Bio-degradable vegetable oil based hyperbranched poly(ester amide) as an advanced surface coating material. *Prog. Org. Coat.* **2013**, *76*, 689−697.

(9) Alam, M.; Sharmin, E.; Ashraf, S. M.; Ahmad, S. Newly developed urethane modified polyetheramide-based anticorrosive coatings from a sustainable resource. *Prog. Org. Coat.* **2004**, *50*, 224−230.

(10) Leila, H.; Xiaohua, K.; Suresh, S. N. Fatty acid-derived diisocyanata and biobased polyurethane produced from vegetable

oil: Synthesis, polymerization, and characterization. *Biomacromolecules* **2009**, *10*, 884−891.
(11) Sarvat, Z.; Uffana, R.; Sharif, A. Water-borne melamine−formaldehyde-cured epoxy−acrylate corrosion resistant coatings. *J. Appl. Polym. Sci.* **2008**, *107*, 215−222.
(12) Saravari, O.; Phapant, P.; Pimpan, V. Synthesis of water-reducible acrylic−alkyd resins based on modified palm oil. *J. Appl. Polym. Sci.* **2005**, *96*, 1170−1175.
(13) Tsujimoto, T.; Uyama, H.; Kobayashi, S. Synthesis of high-performance green nanocomposites from renewable natural oils. *Polym. Degrad. Stab.* **2010**, *95*, 1399−1405.
(14) Yousefi, A. A.; Pishvaei, M.; Yousef, A. Preparation of water-based alkyd/acrylic hybrid resins. *Prog. Color Colorants Coat.* **2011**, *4*, 15−25.
(15) Christian, A.; Goran, S. Multilayered alkyd resin/nanocellulose coatings for use in renewable packaging solutions with a high level of moisture resistance. *Ind. Eng. Chem. Res.* **2013**, *52*, 2582−2589.
(16) Lihui, Z.; Hong, Z.; Jinshan, G. Synthesis and properties of UV curable polyester-based waterborne polyurethane: Functionalization silica composites and morphology of their nanostructured films. *Ind. Eng. Chem. Res.* **2012**, *51*, 8434−8441.
(17) Wang, C.; Jones, F. N. Stability and film properties of tung oil modified soybean alkyd emulsion. *J. Appl. Polym. Sci.* **2000**, *78*, 1698.
(18) Athawale, V. D.; Nimbalkar, R. V. Waterborne coatings based on renewable oil resources: An overview. *J. Am. Oil. Chem. Soc.* **2011**, *88*, 159−185.
(19) Akbarinezhad, E.; Ebrahimi, M.; Kassiriha, S. M.; Khorasani, M. Synthesis and evaluation of water-reducible acrylic−alkyd resins with high hydrolytic stability. *Prog. Org. Coat.* **2009**, *65*, 217−221.
(20) Borah, J.; Mahapatra, S. S.; Saikia, D.; Karak, N. Physical, thermal, dielectric and chemical properties of a hyperbranched polyether and its linear analog. *Polym. Degrad. Stab.* **2006**, *91*, 2911−2916.
(21) Xinbo, S.; Zhengbing, C.; Nuala, P.; Yuyu, S. Amine, melamine, and amide *N*-halamines as antimicrobial additives for polymers. *Ind. Eng. Chem. Res.* **2010**, *49*, 11206−11213.
(22) Chen, Y.; Wilbon, P. A.; Chen, Y. P; Zhou, J.; Nagarkatti, M.; Wang, C.; Chu, F.; Dechob, A. W.; Tang, C. Amphipathic antibacterial agents using cationic methacrylic polymers with natural rosin as pendant group. *RSC Adv.* **2012**, *2*, 10275−10282.
(23) Kenawy, E. R.; Worley, S. D.; Broughton, R. The chemistry and applications of antimicrobial polymers: A state-of-the-art review. *Biomacromolecules* **2007**, *8*, 1359−1384.
(24) Aigbodion, A. I.; Okiemien, F. E.; Obazaa, E. O.; Bakare, I. O. Utilisation of maleinized rubber seed oil and its alkyd resin as binders in water-borne coatings. *Prog. Org. Coat.* **2003**, *46*, 28−31.
(25) Aigbodion, A. I.; Okiemien, F. E.; Ikhuoria, E. U.; Bakare, I. O.; Obazaa, E. O. Rubber seed oil modified with maleic anhydride and fumaric acid and their alkyd resins as binders in water-reducible coatings. *J. Appl. Polym. Sci.* **2003**, *89*, 3256−3259.
(26) Dhoke, S. K.; Khanna, A. S.; Sinha, T. J. M. Effect of nano-ZnO particles on the corrosion behavior of alkyd-based waterborne coatings. *Prog. Org. Coat.* **2009**, *64*, 371−382.
(27) Patton, T. C. *Alkyd Resin Technology*; Interscience Publisher: New York, 1962.
(28) Wang, X.; Wang, J.; Li, Q.; Li, S. Synthesis and characterization of waterborne epoxy−acrylic corrosion-resistant coatings. *J. Macromol. Sci., Part B: Phys.* **2013**, *52*, 751−761.
(29) Dhoke, S. K.; Sinha, T. J. M.; Dutta, P.; Khanna, A. S. Formulation and performance study of low molecular weight, alkyd-based waterborne anticorrosive coating on mild steel. *Prog. Org. Coat.* **2008**, *62*, 183−192.
(30) Ahmad, S.; Ashraf, S. M.; Sharmin, E.; Nazir, M.; Alam, M. Studies on new polyetheramide-butylated melamine formaldehyde based anticorrosive coatings from a sustainable resource. *Prog. Org. Coat.* **2005**, *52*, 85−91.
(31) Radicevic, R.; Jovicic, M.; Simendic, J. B. Preparation and curing of alkyd based on ricinoleic acid/melamine coatings. *Prog. Org. Coat.* **2011**, *71*, 256−264.
(32) Pelezar, M. J.; Chem, C. S.; Reid, R. D. *Microbiology*; McGraw Hill: New York, 1990.
(33) Elmorsi, M. A.; Issa, R. M. Corrosion of metal pipes in ground water. *B. Electrochem.* **1988**, *4*, 785−788.
(34) Nimbalkar, R. V.; Athawale, V. D. Synthesis and characterization of canola oil alkyd resins based on novel acrylic monomer (ATBS). *J. Am. Oil Chem. Soc.* **2010**, *87*, 947−954.
(35) Farber, I. Y.; Beyth, N.; Weiss, E. I.; Domb, A. J. Antibacterial effect of composite resins containing quaternary ammonium polyethyleneimine nanoparticles. *J. Nanopart. Res.* **2010**, *12*, 591−603.
(36) Spyros, A. Characterization of unsaturated polyester and alkyd resins using one- and two-dimensional NMR spectroscopy. *J. Appl. Polym. Sci.* **2003**, *88*, 1881−1888.
(37) Pavia, D. L.; Lampman, G. M.; Kriz, G. S.; Vyvyan, J. R. *Spectroscopy*; Cengage Learning: Canada, 2007.
(38) Karak, N.; Roy, B.; Voit, B. s-Triazine-based hyperbranched polyethers: Synthesis, characterization and properties. *J. Polym. Sci., Part A: Polym. Chem.* **2010**, *48*, 3994−4004.
(39) Mahapatra, S.; Karak, N. Fluorescent hyperbranched polyamine with *s*-triazine: Synthesis, characterization and properties evaluation. *Polym. J.* **2009**, *41*, 20−25.
(40) Konwar, U.; Karak, N. Hyperbranched polyether core containing vegetable oil-modified polyester and its clay nano-composites. *Polym. J.* **2011**, *43*, 565−576.
(41) Ahmad, S.; Ashraf, S. M.; Kumar, G. S.; Hasnat, A.; Sharmin, E. Studies on epoxy-butylated melamine formaldehyde-based anticorrosive coatings from a sustainable resource. *Prog. Org. Coat.* **2006**, *56*, 207−213.
(42) Weng, C. J.; Chang, C. H.; Peng, C. W.; Chen, S. W.; Yeh, J. M.; Hsu, C. L.; Wei, Y. Advanced anticorrosive coatings prepared from the mimicked xanthosoma sagittifolium-leaf-like electroactive epoxy with synergistic effects of superhydrophobicity and redox catalytic capability. *Chem. Mater.* **2011**, *23*, 2075−2083.
(43) De, B.; Karak, N. Novel high performance tough hyperbranched epoxy by an A2 + B3 polycondensation reaction. *J. Mater. Chem. A.* **2013**, *1*, 348−353.
(44) Akshya, K. G.; Suryakanta, N.; Tapan, K. R.; Nikhiles, B.; Dillip, K. S. Corrosion resistance nano-hybrid sol-gel coating on steel sheet. *ISIJ Int.* **2011**, *51*, 435−440.
(45) Narayan, R.; Chattopadhyay.; Sreedhar, B.; Raju, V. S. N. Cure, viscoelastic and mechanical properties of hydroxylated polyester melamine high solids coatings. *J. Mater. Sci.* **2002**, *37*, 4911−4918.
(46) Pan, X.; Sengupta, P.; Webster, D. C. High biobased content epoxy−anhydride thermosets from epoxidized sucrose esters of fatty acids. *Biomacromolecules* **2011**, *12*, 2416−2428.
(47) Sarvat, Z.; Fahmina, Z.; Ufana, R.; Sharif, A. Synthesis, characterization, and anticorrosive coating properties of waterborne interpenetrating polymer network based on epoxy-acrylic-oleic acid with butylated melamine formaldehyde. *J. Appl. Polym. Sci.* **2009**, *113*, 827−838.
(48) Chattopadhyay, D. K.; Webster, D. C. Thermal stability and flame retardancy of polyurethanes. *Prog. Polym. Sci.* **2009**, *34*, 1068−1133.
(49) Zhou, Y.; Min, J.; Lui, Z.; Young, H.; Deshazer, H.; Gao, T.; Chang, T. C.; Kallenbach, N. R. Synthesis and biological evaluation of novel 1,3,5-triazine derivatives as antimicrobial agents. *Bioorg. Med. Chem. Lett.* **2008**, *18*, 1308−1311.
(50) Dizman, B.; Elasri, M. O.; Mathias, L. J. Synthesis, characterization, and antibacterial activities of novel methacrylate polymers containing norfloxacin. *Biomacromolecules* **2005**, *6*, 514−520.
(51) Timofeeva, L. M.; Kleshcheva, N. A.; Moroz, A. F.; Didenko, L. V. Secondary and tertiary polydiallylammonium salts: Novel polymers with high antimicrobial activity. *Biomacromolecules* **2009**, *10*, 2976−2986.
(52) Yang, T.; Peng, C. W.; Lin, Y. L.; Weng, C. J.; Edgington, G.; Mylonakis, A.; Huang, T. C.; Hsu, C. H.; Yeh, J. M.; Wei, Y. Synergistic effect of electroactivity and hydrophobicity on the anticorrosion property of room-temperature-cured epoxy coatings

with multi-scale structures mimicking the surface of *Xanthosoma sagittifolium* leaf. *J. Mater. Chem.* **2012**, *22*, 15845−15852.
(53) Shukla, S. K.; Singh, A. K.; Quraishi, M. A. Triazines: Efficient corrosion inhibitors for mild steel in hydrochloric acid solution. *Int. J. Electrochem. Sci.* **2012**, *7*, 3371−3389.
(54) Phanasgaonkar, A.; Raja, V. S. Influence of curing temperature, silica nanoparticles and cerium on surface morphology and corrosion behaviour of hybrid silane coatings on mild steel. *Surf. Coat. Technol.* **2009**, *203*, 2260−2271.
(55) Ahmad, S.; Zafar, F.; Sharmin, E.; Garg, N.; Kashif, M. Synthesis and characterization of corrosion protective polyurethanefattyamide/silica hybrid coating material. *Prog. Org Coat.* **2012**, *73*, 112−117.
(56) Wang, Y. B.; Li, H. F.; Zheng, Y. F.; Wei, S. C.; Li, M. Correlation between corrosion performance and surface wettability in ZrTiCuNiBe bulk metallic glasses. *Appl. Phys. Lett.* **2010**, *96*, 251909−1.
(57) Peng, C. W.; Chang, K. C.; Weng, C. J.; Lai, M. C.; Hsu, C. H.; Hsu, S. C.; Li, S. Y.; Weib, Y.; Yeh, J. M. UV-curable nanocasting technique to prepare bio-mimetic super-hydrophobic non-fluorinated polymeric surfaces for advanced anticorrosive coatings. *Polym. Chem.* **2013**, *4*, 926−932.
(58) Yadav, D. K.; Chauhan, D. S.; Ahamad, I.; Quraishi, M. A. Electrochemical behavior of steel/acid interface: adsorption and inhibition effect of oligomeric aniline. *RSC Adv.* **2013**, *3*, 632−646.
(59) Mahdavian, M.; Ashhari, S. Corrosion inhibition performance of 2-mercaptobenzimidazole and 2-mercaptobenzoxazole compounds for protection of mild steel in hydrochloric acid solution. *Electrochim. Acta* **2010**, *55*, 1720−1724.
(60) Ahamad, I.; Quraishi, M. A. Mebendazole: New and efficient corrosion inhibitor for mild steel in acid medium. *Corros. Sci.* **2010**, *52*, 651−656.
(61) Zang, R. Z.; langroudi, A. E; Rahimi, A. Silica based organic−inorganic hybrid nanocomposite coatings for corrosion protection. *Prog. Org. Coat.* **2005**, *53*, 286−291.
(62) Zheludkevich, M. L.; Salvodo, I. M.; Ferreira, M. G. S. Sol−gel coatings for corrosion protection of metals. *J. Mater. Chem.* **2005**, *15*, 5099−5111.